PHATNet: A Physics-guided Haze Transfer Network for Domain-adaptive Real-world Image Dehazing
Supplementary Material

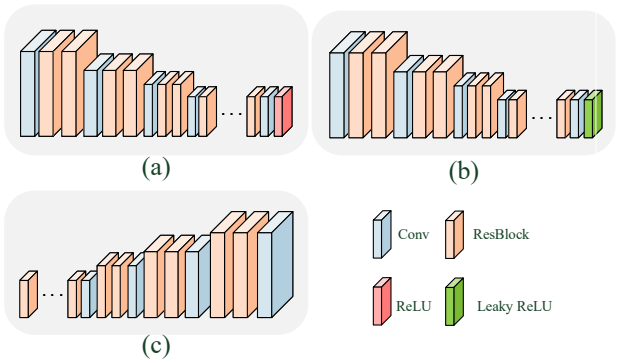

Figure 1. (a) Architectures of Atmospheric Light Encoder (ALE) and Transmission Maps Encoder (TME). (b) Architectures of Content Encoder (CE). (c) Architectures of Rehazing Encoder (RE).

1. Justifying why haze patterns are easy to learn

To validate this observation, we compare the dehazing and rehazing performances using the FocalNet backbone. Trained on NH-Haze20, FocalNet learns dehazing (hazy-to-clean) and rehazing (clean-to-hazy) tasks. The training PSNR is 25.62 dB for dehazing and 30.33 dB for rehazing, indicating learning haze patterns is easier than restoring clean content.

2. Architectures of ALE, TME, CE, and RE

In Figure 1, we provide the architectures of Atmospheric Light Encoder (ALE), Transmission Maps Encoder (TME), Content Encoder (CE), and Rehazing Encoder (RE). The ALE, TME, and CE encoders all adopt a four-stage structure with channel sizes of 16, 32, 64, and 128, respectively. In the first three stages, each encoder consists of a convolutional layer followed by two ResBlocks, while the final stage has a convolutional layer followed by six ResBlocks. For ALE and TME, the ReLU activation function is applied at the end of the encoder to guarantee positive output values for the atmospheric light and transmission magnitude, as shown in Figure 1 (a). In contrast, for CE, we use the Leaky ReLU activation function at the end of the encoder to preserve more content information, as depicted in Figure 1 (b). For RE, as shown in Figure 1(c), we use a four-stage structure with channel sizes of 128, 64, 32, and 16, respectively. The first stage consists of six ResBlocks followed by a convolutional layer, while the last three stages stack two ResBlocks, followed by a convolutional layer.

Figure 2. Illustration of PHDT-based hazy image augmentation. Beyond generating the haze-transferred image, we can vertically flip F^{TM} to augment image A, rotate F^{TM} to augment image B, and invert F^{TM} using 1 - F^{TM} to augment image C.

3. Image Counts in the Fine-tuning Sets

As mentioned in Section 3.4, we use PHATNet to transfer haze patterns from hazy images $\{\tilde{I}_i^H\}_{i=1}^M$ in the target domain to haze-free images $\{I_j^C\}_{j=1}^N$ in the source domain, producing a domain-specific fine-tuning set $S = \{\tilde{I}_{i,j}^O, I_j^C\}$ with a total of $M \times N$ training pairs.

In **Setting1**, we use NHHaze20, with 50 haze-free images, as the source domain and NH-Haze21, HD-NH-Haze, DenseHaze, I-Haze, O-Haze, and RTTS datasets as target domains, with 25, 40, 55, 30, 40, 4322 hazy images, respectively. We generate $1,250$, $2,000$, $2,750$, $1,500$, $2,000$, and $216,100$ haze-transferred images for NH-Haze21, HD-NH-Haze, DenseHaze, I-Haze, O-Haze, and RTTS datasets, respectively.

In **Setting2**, we use HD-NH-Haze, with 35 haze-free images, as the source domain and NH-Haze20, NH-Haze21, DenseHaze, I-Haze, O-Haze, and RTTS datasets as target domains, with 55, 25, 55, 30, 40, $4,322$ hazy images, respectively. We generate $1,925$, 875, $1,925$, $1,050$, $1,400$,

and $151,270$ haze-transferred images for NH-Haze20, NH-Haze21, DenseHaze, I-Haze, O-Haze, and RTTS datasets, respectively.

4. Discussions of hazy image augmentation

In Figure 2, we manipulate the haze-transferred images in the ASM parametric domain to create additional target-domain hazy images. We adjust the haze distribution by modifying the transmission-map features F^{TM} to generate augmented images with varying haze effects. Specifically, we vertically flip F^{TM} to create vertically flipped haze, as shown in Augmented Image A, , or rotate F^{TM} to produce rotated haze, as illustrated in Augmented Image B. When applying the inverse transmission-map features $\tilde{F}^{\mathrm{TM}}$ = 1 - F^{TM}, the resulting hazy image appears noticeably less realistic, as shown in Augmented Image C. This occurs because the inverse transmission features in originally haze-free regions approach zero, resulting in an overly uniform haze effect that lacks the diffused, misty, and naturally irregular characteristics of real haze. Consequently, synthesizing realistic hazy images by manually defining haze distributions remains a significant challenge.

5. Discussions of using a limited amount of training data

While PHATNet is optimized using a limited number of hazy-clean image pairs, the training hazy images effectively capture diverse hazy patterns due to the high regularity and smoothness of real haze in the ASM parametric domain. To address the greater diversity of scene content, we further enhance the training process by incorporating unpaired haze-free images through the Content-Leakage (CL) loss. This approach significantly augments the training dataset, ensuring ample samples to fine-tune PHATNet and enhance its overall performance.

6. Visualization results of dehazed images

We present dehazed images produced with and without using PHATNet-augmented data under **Setting1** in Figures 3 to 10 and under **Setting2** in Figures 11 to 18. For **Setting1**, we present dehazed results of FocalNet [7] on HD-NH-Haze [6] and RTTS [10] datasets in Figures 3 and 4, dehazed results of Dehamer [9] on HD-NH-Haze [6] and RTTS [10] datasets in Figures 5 and 6, dehazed results of MITNet [11] on NH-Haze21 [5] and RTTS [10] datasets in Figures 7 and 8, and dehazed results of SGDN [8] on NH-Haze21 [5] and RTTS [10] datasets in Figures 9 and 10. For **Setting2**, we present dehazed results of FocalNet [7] on NH-Haze20 [4] and RTTS [10] datasets in Figure 11 and Figure 12, dehazed results of Dehamer [9] on I-Haze [1] and DenseHaze [3] in Figure 13 and RTTS [10] datasets in Figure 14, dehazed results of MITNet [11] on O-Haze [2] and RTTS [10] datasets in Figures 15 and 16, and dehazed results of SGDN [8] on O-Haze [2] and RTTS [10] datasets in Figures 17 and 18. These visualization results showcase PHATNet's capability to enhance visual quality for domain adaptation.

7. Results of haze-transferred images

We present haze-transferred images under **Setting1** in Figure 19 and under **Setting2** in Figure 20. PHATNet effectively transfers haze patterns to various haze-free images, generating hazy images with consistent haze patterns but different content. This demonstrates PHATNet's ability to reliably transfer haze patterns across different haze-free images.

References

[1] Codruta O. Ancuti, Cosmin Ancuti, Radu Timofte, and Christophe De Vleeschouwer. I-HAZE: a dehazing benchmark with real hazy and haze-free indoor images. In *ACIVS*, 2018. 2, 13

[2] Codruta O. Ancuti, Cosmin Ancuti, Radu Timofte, and Christophe De Vleeschouwer. O-HAZE: a dehazing benchmark with real hazy and haze-free outdoor images. In *CVPRW*, 2018. 2, 15, 17

[3] Codruta O. Ancuti, Cosmin Ancuti, Mateu Sbert, and Radu Timofte. Dense-Haze: A benchmark for image dehazing with dense-haze and haze-free images. In *ICIP*, 2019. 2, 13

[4] Codruta O. Ancuti, Cosmin Ancuti, and Radu Timofte. NH-HAZE: an image dehazing benchmark with non-homogeneous hazy and haze-free images. In *CVPRW*, 2020. 2, 11, 19

[5] Codruta O. Ancuti, Cosmin Ancuti, Florin-Alexandru Vasluianu, and Radu Timofte. Ntire 2021 nonhomogeneous dehazing challenge report. In *CVPRW*, 2021. 2, 7, 9, 20

[6] Codruta O. Ancuti, Cosmin Ancuti, Florin-Alexandru Vasluianu, and Radu Timofte. Ntire 2023 hr nonhomogeneous dehazing challenge report. In *CVPRW*, 2023. 2, 3, 5, 19, 20

[7] Yuning Cui, Wenqi Ren, Xiaochun Cao, and Alois Knoll. Focal network for image restoration. In *ICCV*, 2023. 2, 3, 4, 11, 12

[8] Wenxuan Fang, JunKai Fan, Yu Zheng, Jiangwei Weng, Ying Tai, and Jun Li. Guided real image dehazing using ycbcr color space. In *AAAI*, 2025. 2, 9, 10, 17, 18

[9] Chun-Le Guo, Qixin Yan, Saeed Anwar, Runmin Cong, Wenqi Ren, and Chongyi Li. Image dehazing transformer with transmission-aware 3d position embedding. In *CVPR*, 2022. 2, 5, 6, 13, 14

[10] Boyi Li, Wenqi Ren, Dengpan Fu, Dacheng Tao, Dan Feng, Wenjun Zeng, and Zhangyang Wang. Benchmarking single-image dehazing and beyond. *IEEE TIP*, 2019. 2, 4, 6, 8, 10, 12, 14, 16, 18

[11] Hao Shen, Zhong-Qiu Zhao, Yulun Zhang, and Zhao Zhang. Mutual information-driven triple interaction network for efficient image dehazing. In *ACM MM*, 2023. 2, 7, 8, 15, 16

Figure 3. Qualitative results of FocalNet [7] on HD-NH-Haze [6] dataset.

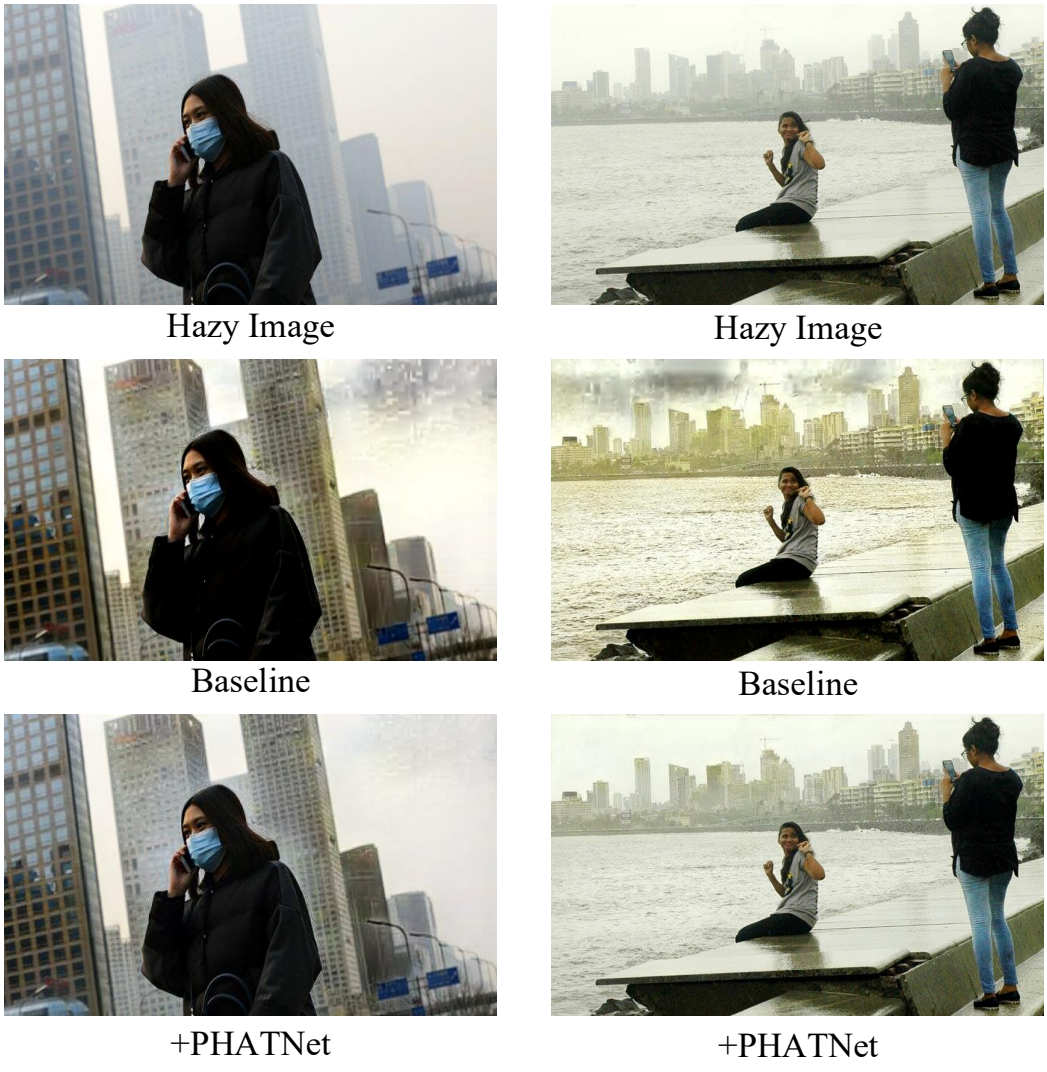

Figure 4. Qualitative results of FocalNet [7] on RTTS [10] dataset.

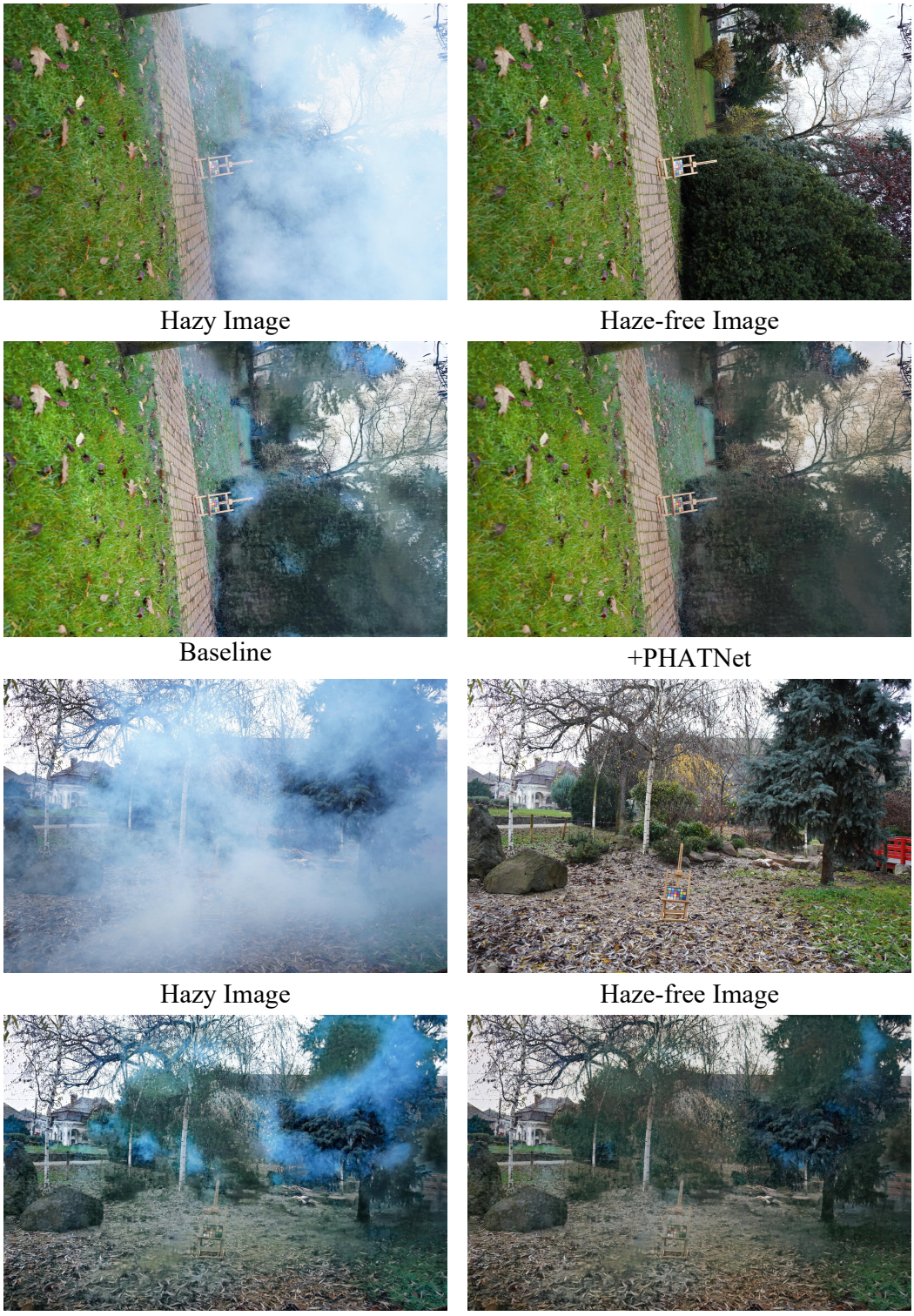

Figure 5. Qualitative results of Dehamer [9] on HD-NH-Haze [6] dataset.

Hazy Image

Hazy Image

Baseline

Baseline

+PHATNet

+PHATNet

Figure 6. Qualitative results of Dehamer [9] on RTTS [10] dataset.

Hazy Image | Haze-free Image

Baseline | +PHATNet

Hazy Image | Haze-free Image

Baseline | +PHATNet

Figure 7. Qualitative results of MITNet [11] on NH-Haze21 [5] dataset.

Hazy Image

Hazy Image

Baseline

Baseline

+PHATNet

+PHATNet

Figure 8. Qualitative results of MITNet [11] on RTTS [10] dataset.

Figure 9. Qualitative results of SGDN [8] on NH-Haze21 [5] dataset.

Hazy Image

Hazy Image

Baseline

Baseline

+PHATNet

+PHATNet

Figure 10. Qualitative results of SGDN [8] on RTTS [10] dataset.

Hazy Image | Haze-free Image

Baseline | +PHATNet

Hazy Image | Haze-free Image

Baseline | +PHATNet

Figure 11. Qualitative results of FocalNet [7] on NH-Haze20 [4] dataset.

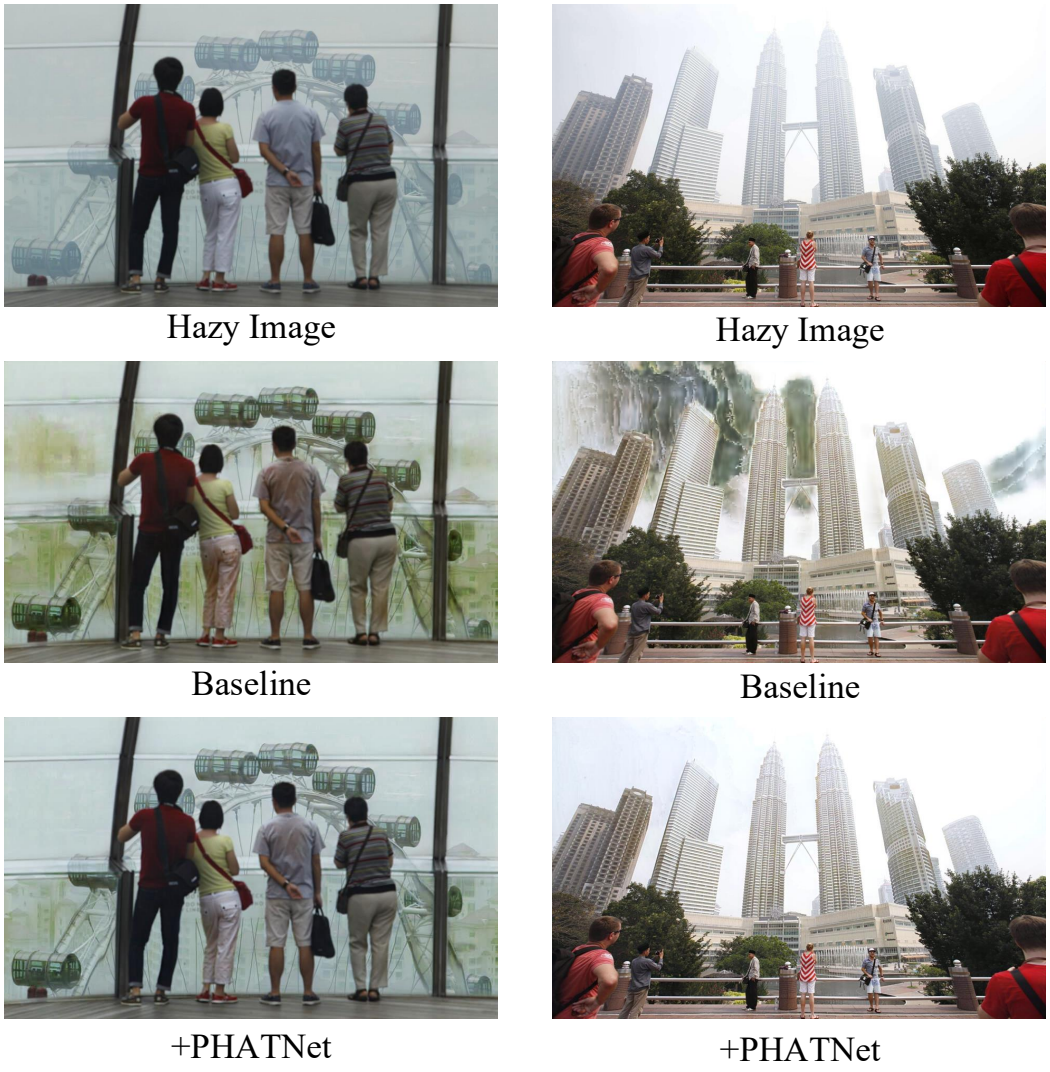

Figure 12. Qualitative results of FocalNet [7] on RTTS [10] dataset.

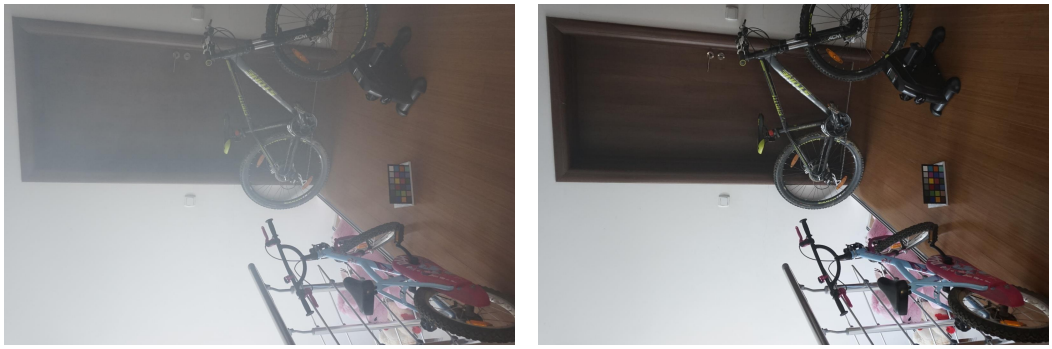

Hazy Image | Haze-free Image

Baseline | +PHATNet

Hazy Image | Haze-free Image

Baseline | +PHATNet

Figure 13. Qualitative results of Dehamer [9] on I-Haze [1] and DenseHaze [3] datasets.

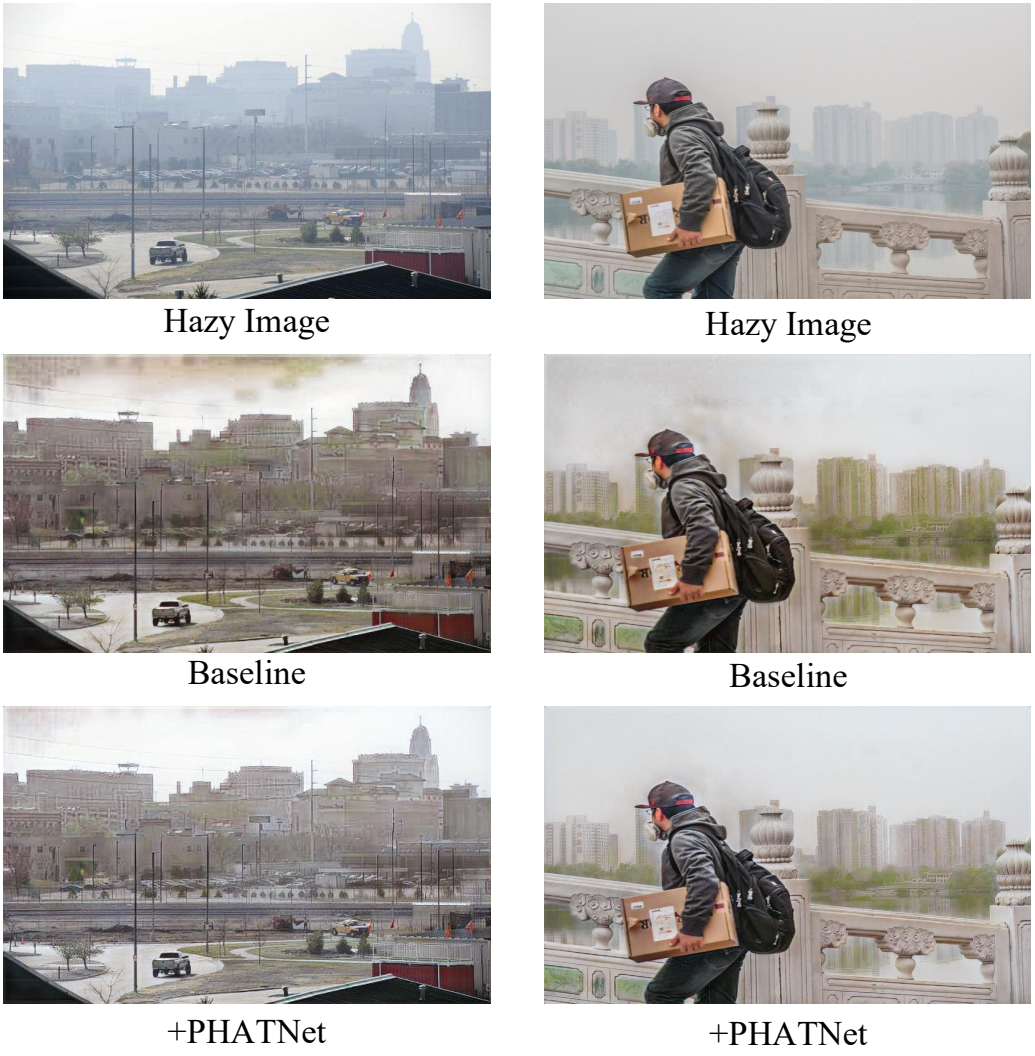

Figure 14. Qualitative results of Dehamer [9] on RTTS [10] datasets.

Hazy Image | Haze-free Image

Baseline | +PHATNet

Hazy Image | Haze-free Image

Baseline | +PHATNet

Figure 15. Qualitative results of MITNet [11] on O-Haze [2] datasets.

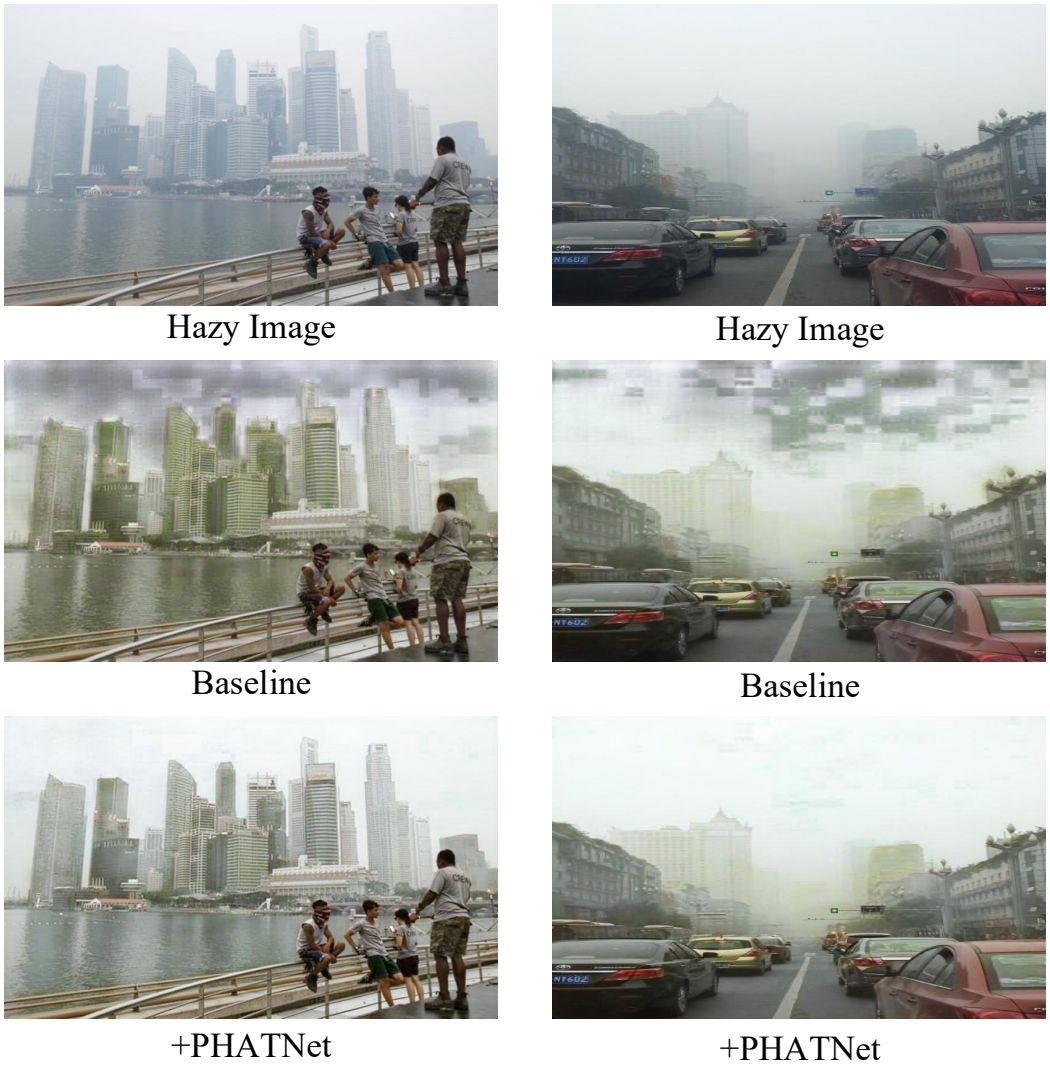

Figure 16. Qualitative results of MITNet [11] on RTTS [10] datasets.

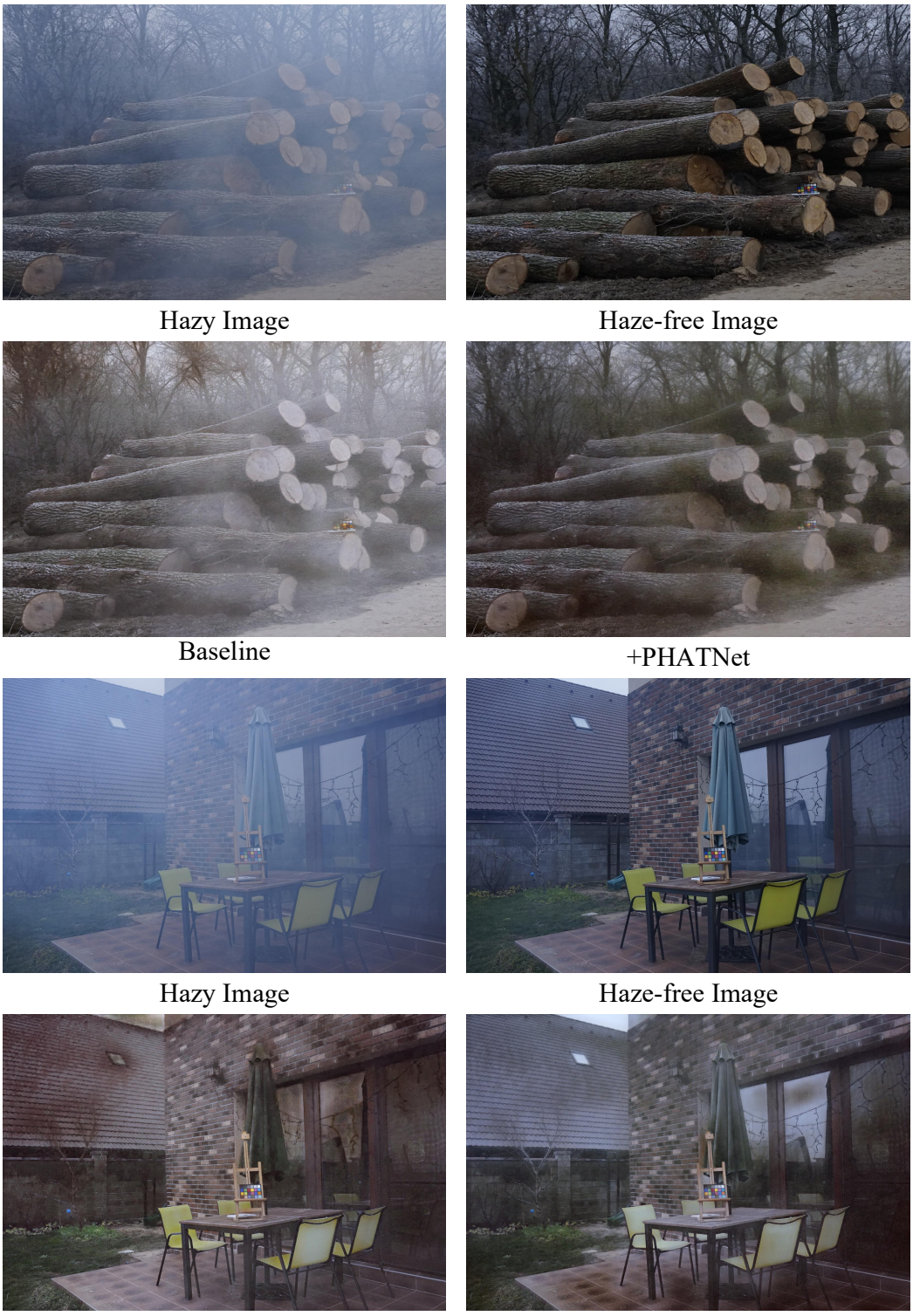

Figure 17. Qualitative results of SGDN [8] on O-Haze [2] dataset.

Hazy Image

Hazy Image

Baseline

Baseline

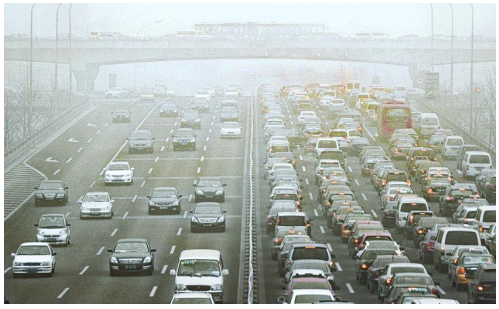

+PHATNet

+PHATNet

Figure 18. Qualitative results of SGDN [8] on RTTS [10] dataset.

Hazy Image

Haze-free Image Haze-transferred Image

Figure 19. Qualitative results of haze-transferred images. We transfer haze patterns from HD-NH-Haze [6] to haze-free images from NH-Haze20 [4].

Hazy Image

Haze-free Image Haze-transferred Image

Figure 20. Qualitative results of haze-transferred images. We transfer haze patterns from NH-Haze21 [5] to haze-free images from HD-NH-Haze [6].